Fractures in healthy females followed from childhood to early adulthood are associated with later menarcheal age and with impaired bone microstructure at peak bone mass

Fractures in Healthy Females Followed from Childhood to Early Adulthood Are Associated with Later Menarcheal Age and with Impaired Bone Microstructure at Peak Bone Mass

T. Chevalley, J. P. Bonjour, B. van Rietbergen, R. Rizzoli, and S. Ferrari

Division of Bone Diseases (T.C., J.P.B., R.R., S.F.), University Hospitals and Faculty of Medicine, CH-1211 Geneva, Switzerland; and Department of Biomedical Engineering (B.v.R.), Eindhoven University of Technology, 5600 MB Eindhoven, The Netherlands

Background: Whether fractures observed in healthy children are associated with microstructural alterations and strength deficit that persists by the end of the growth period is not established. Considering the importance of pubertal timing in bone development, we also quantified the fracture risk related to later menarcheal age (MENA).

Participants and Methods: We followed 124 healthy girls from mean $\pm$ sd age 7.9 $\pm$ 0.5 to 20.4 $\pm$ 0.6 yr. Fractures, MENA, and radius areal bone mineral density (aBMD) were recorded at regular intervals. At a mean age of 20.4 yr, microstructural and strength variables of the distal radius were determined by high-resolution peripheral computerized tomography and micro-finite element analysis.

Results: Sixty-one fractures occurred in 42 subjects. At 20.4 yr, subjects with fractures had lower aBMD at radial diaphysis ($P = 0.005$) and metaphysis ($P = 0.008$), lower distal radius trabecular volumetric density (vBMD) ($P = 0.010$) and thickness ($P = 0.014$), and reduction in stiffness ($P = 0.013$), failure load ($P = 0.013$), and apparent modulus ($P = 0.046$). Odds ratios revealed an increased risk of fracture for a 1-sd reduction in radial aBMD diaphysis [1.97 ($P = 0.006$)] and metaphysis [1.97 ($P = 0.008$)] and distal radius trabecular vBMD [1.89 ($P = 0.011$)], thickness [1.97 ($P = 0.017$)], stiffness [2.02 ($P = 0.014$)], failure load [2.00 ($P = 0.014$)], and apparent modulus [1.79 ($P = 0.043$)]. MENA occurred at a later age in subjects with fractures ($P = 0.003$). For MENA 1 sd (1.2 yr) later, the increase of fracture risk was 2.1 ($P = 0.002$).

Conclusions: In healthy young women, low trabecular vBMD and thickness in the distal radius are associated with reduced bone strength and increased fracture risk during growth. This study also documents that later pubertal timing is associated with increased incidence of fracture during childhood and adolescence. (*J Clin Endocrinol Metab* 97: 4174–4181, 2012)

Fractures are frequently observed in healthy children and adolescents, with an increased prevalence at peak height velocity (1–6). This relationship has been ascribed to a period of transient fragility resulting from an asynchrony between the rate of longitudinal growth and that of bone accumulation (7, 8). This transient fragility has also been suggested to be due to an increased bone porosity (9). This notion has recently found some support by using high-resolution imaging allowing one to quantify both the number and size of pores in the forearm cortex of adolescents (10), but so far, no study has compared bone porosity at or close to peak bone mass attainment between subjects with or without a positive history of fractures.

Abbreviations: aBMD, Areal bone mineral density; CI, confidence interval; DXA, dual-energy x-ray absorptiometry; μFEA, micro-finite element analysis; FX group, group with fracture; HA, hydroxyapatite; HR-pQCT, high-resolution peripheral quantitative computerized tomography; MENA, menarcheal age; NO-FX group, group without fracture; OR, odds ratio; vBMD, volumetric BMD.

Fracture data only recorded from 7.9–16.4 yr in the cohort studied in the following report was previously discussed in relation to bone mineral content gain in the radial metaphysis, as assessed by dual-energy x-ray absorptiometry (DXA) (11). This previous report did not include any microstructure component analysis or strength estimates. It suggested that a deficit in the radius observed in prepuberty and at a mean age of 16.4 yr could not only be related to the incidence of forearm fracture during growth but also may be a marker for lower peak bone mass attainment and thereby be a risk factor for osteoporosis in adulthood (11). Furthermore, this increased risk of fracture during growth could still be influenced by the timing of pubertal maturation, the impact of which on bone acquisition is detectable from 5 yr before menarche until the time of peak bone mass attainment, as previously reported in our cohort of healthy young adult women (12). In this cohort, a 1.9-yr difference in mean menarcheal age (MENA) was associated not only with lower radial areal bone mineral density (aBMD) T-score but also with lower total volumetric BMD (vBMD), cortical vBMD, and cortical thickness at the distal radius (13). This set of independent observations raises the ancillary question of whether the incidence rate of fracture would be influenced by the timing of pubertal maturation that appears to be linked to bone mineral mass accumulation and risk of fracture during development (14), as previously documented in a healthy male cohort (15).

In the present report, we tested these two related hypotheses in a prospective longitudinal study in our cohort of healthy female subjects followed from a mean age of 7.9 to 20.4 yr, *i.e.* until an age there was quantitative evidence the subjects had reached peak bone mass.

Therefore, we analyzed at a mean age of 20.4 yr the distribution of fractures recorded during childhood and adolescence until peak bone mass attainment and studied in addition to DXA measurement whether some of the distal radius microstructure components including porosity and strength estimates as assessed by high-resolution peripheral quantitative computerized tomography (HR-pQCT) and micro-finite element analysis (μFEA), respectively, were related to the risk of fracture during skeletal development. We also examined to what extent pubertal timing, as precisely assessed by prospectively recording MENA, modulated the risk of fracture throughout the period of bone acquisition.

Subjects and Methods

Participants

Fracture history and BMD and cortical and trabecular microstructure as well as bone strength estimates assessed by HR-

pQCT and μFEA were studied in a cohort of 124 healthy young adult women at a mean age of 20.4 ± 0.6 (±SD) yr. Influence of age at menarche on forearm microstructure has been previously reported in this cohort (13). These women belonged to a cohort followed for 12 yr and previously examined for the first time at a mean age of 7.9 ± 0.5 yr (16) and then successively at mean age of 8.9 ± 0.5, 9.9 ± 0.5 (16), 12.4 ± 0.5 (17), and 16.4 ± 0.5 yr (18). After enrollment at a mean age of 7.9 ± 05 yr, half of the cohort received during 1 yr a supplementation of calcium in a randomized, double-blind, placebo-controlled design as previously reported (16). The ethics committees of the Department of Pediatrics and the Department of Rehabilitation and Geriatrics of the University Hospitals of Geneva approved the protocol, and informed consent was obtained from both parents and children (16). All subjects were recruited within the Geneva area, and exclusion criteria at baseline were weight to height ratio below the third or above the 97th percentile, physical signs of puberty, chronic disease, malabsorption, bone disease, and regular use of medication.

Clinical assessment

Body weight, standing height, and body mass index (kilograms per square meter) were prospectively measured at each visit. During the first two visits at mean age ± SD 7.9 ± 0.5 and 8.9 ± 0.5 yr, pubertal stage was assessed by direct clinical examination made by a pediatrician-endocrinologist. At mean age of 10.0, 12.4, and 16.4 yr, pubertal maturation was assessed by a self-assessment questionnaire with drawings and written description of Tanner's breast and pubic hair. At the time of the first two visits at a mean age of 7.9 and 8.9 yr, all girls were classified Tanner's stage P1, whereas at mean age of 10.0 yr, 38% of them had reached Tanner's stage P2. MENA was then assessed prospectively by direct interview at the second, third, fourth, and fifth visits, *i.e.* at the mean age of 8.9, 10.0, 12.4, and 16.4 yr. Fracture history since birth, including skeletal site, year of event, and type of intervention, was recorded for the first time at a mean age of 7.9 yr and then at each follow-up visit from the children and their parents.

Calcium and protein intake assessment

Calcium intake was estimated mostly from dairy sources by a frequency questionnaire at each visit from a mean age of 7.9 yr (19). Protein intake was assessed by frequency questionnaire (20) at the mean age of 20.4 y. The total animal protein intake was expressed either in grams per day or grams per kilogram body weight per day. It included dairy, meat, fish, and egg proteins.

Physical activity assessment

Physical activity in these young adult women was assessed by a questionnaire based on self-reported time spent in physical education classes, organized sports, recreational activity, and usual walking and cycling (21). Subsequently, the collected data were converted and expressed as physical activity energy expenditure (kilocalories per day) using established conversion formulas (22).

Measurement of bone variables

The aBMD was determined by DXA using a Hologic QDR 4500 instrument (Waltham, MA) at the radial metaphysis and diaphysis in anteroposterior view as previously reported (13). The coefficient of variation of repeated measurements at these

sites, as determined in young healthy adults, varied from 1.0–1.6% for BMD.

The vBMD and microstructure were determined at the distal radius by HR-pQCT with an XtremeCT instrument (Scanco Medical AG, Bassersdorf, Switzerland) that acquires a stack of 110 parallel computerized tomography slices (9-mm length) with an isotropic voxel size of 82 μm as previously described (13, 23). Unless there was a history of fracture, DXA and HR-pQCT measurements were performed on the nondominant forearm. The following variables were measured: total, cortical, and trabecular vBMD expressed as milligrams hydroxyapatite (HA) per cubic centimeter; trabecular bone volume fraction (percent); trabecular number, thickness, and spacing (micrometers); and mean cortical thickness (micrometers) and cross-sectional area (square millimeters).

The HR-pQCT images were filtered and binarized using the standard manufacturer's method (24). The periosteal and endosteal boundaries were defined using an automated contouring method similar to the technique described previously by Buie and colleagues (25) as implemented in Image Processing Language (IPL version 5.07; Scanco Medical). The automated segmentation uses two threshold values and a series of morphological operations (*e.g.* dilation and erosion operations) to extract the endosteal and periosteal surfaces of the cortex and was validated earlier (26, 27).

Cortical porosity (percent) was calculated as the number of void voxels in each binary cortex image divided by the total number of voxels (27). The *in vivo* short-term reproducibility of HR-pQCT at the distal radius assessed in 15 subjects with repositioning varied from 0.6–1.0% and from 2.8–4.9% for bone density and for trabecular structure, respectively. These reproducibility ranges are similar to those previously published (28). One technician per device performed all the scans as well as daily quality control phantom to check for possible drifts in the x-ray sources.

Finite element analysis

The finite element model of the radius was created directly from the segmented HR-pQCT images using a procedure similar to that used in earlier clinical studies (29–31). In summary, a voxel-conversion procedure was used to convert each voxel of bone tissue into an equally sized brick element (32), thus creating μFE models that can represent the actual trabecular architecture in detail. The models contained approximately 2 million elements for the radius and could be solved in approximately 3 h. Material properties isotropic and elastic were chosen. Both cortical and trabecular bone elements were assigned a Young's modulus of 10 and a Poisson's ratio of 0.3 (30, 33). A compression test was simulated to represent loading conditions during a fall from standing height (34). Bone failure load was calculated as the force for which 2% of the bone tissue would be loaded beyond 0.7% strain (33, 35). In addition to failure load (Newtons), μFEA-derived variables used in our study also included stiffness kilo-Newtons per millimeter). All μFE analyses were done using the FE solver integrated in the IPL software version 1.15 (Scanco Medical).

Expression of the results and statistical analysis

The various anthropometric and osteodensitometric variables are given as mean ± SD. The T-score based on the value used in the clinical unit dedicated to the diagnosis of osteoporosis at the University Hospital of Geneva (13, 36) was used to assess whether the cohort mean value with a 95% confidence interval (CI) of radial aBMD could be considered at peak bone mass. The

differences in density, microstructure, mechanical parameters, and clinical characteristics among participants with or without a positive history of fracture were assessed by unpaired Student's *t* test or by Wilcoxon signed rank test whenever the variable was not normally distributed. Pearson's correlation coefficients R were calculated for the relationships between cortical porosity and cortical vBMD and thickness. For the differences in density, microstructure, and mechanical parameters between fracture and nonfracture subjects, an analysis of covariance was used to control the influence of age, height, weight, MENA, calcium and protein intake, physical activity, and calcium supplement or placebo randomization between the mean age of 7.9 and 8.9 yr. Associations between density, microstructure, mechanical parameters, and fracture status were evaluated by logistic regression analysis with adjustment for age, height, weight, MENA, calcium and protein intake, physical activity, and calcium supplement or placebo randomization between the mean age of 7.9 and 8.9 yr and expressed as odds ratio (OR) with 95% CI per SD decrease. The significance level for two-sided *P* values was 0.05 for all tests. The data were analyzed using STATA software version 9.2. (StataCorp LP, College Station, TX).

Results

Characteristics of the cohort

Anthropometric data and dietary intake (calcium and proteins) as well as physical activity did not differ between the group with fracture (FX) (n = 42) and the group without fracture (NO-FX) (n = 82) (Table 1). The proportion

TABLE 1. Characteristics of healthy young adult women according to their fracture history

	All (n = 124)	NO-FX (n = 82)	FX (n = 42)
Age (yr)	20.4 ± 0.6	20.39 ± 0.58	20.42 ± 0.63
MENA (yr)	13.0 ± 1.2	12.78 ± 1.19	13.45 ± 1.11[a]
Height (cm)	165.0 ± 6.0	165.0 ± 6.1	164.8 ± 6.5
Weight (kg)	60.0 ± 9.2	59.2 ± 8.3	61.4 ± 10.8
Body mass index (kg/m²)	22.1 ± 3.4	21.8 ± 2.9	22.7 ± 4.1
Calcium intake (mg/d)	832 ± 380	807 ± 374	879 ± 390
Protein intake (g/d)	41.6 ± 16.7	40.3 ± 16.7	44.0 ± 16.7
Protein intake (g/kg BW · d)	0.71 ± 0.31	0.69 ± 0.32	0.74 ± 0.30
Physical activity (kcal/d)	352 ± 298	347 ± 246	362 ± 384
Calcium supplement (n)/placebo (n)[b]	65/59	46/36	19/23

Values are means ± SD as determined by the end of the follow-up study, *i.e.* at the last study visit. BW, Body weight.

[a] *P* = 0.003 as compared with young adult women without fracture.

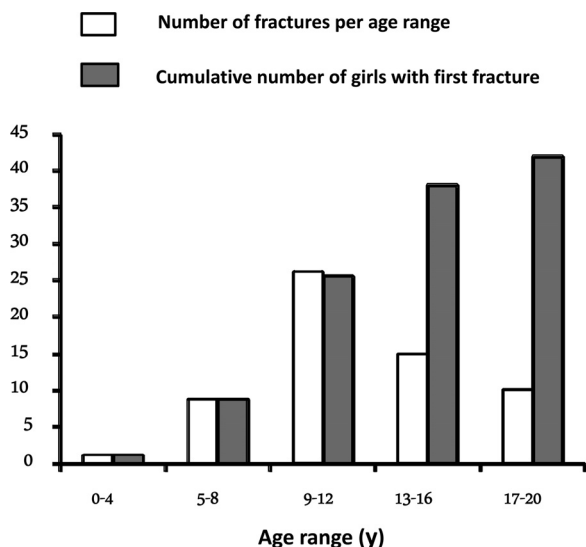[b] Calcium or placebo randomization between mean age of 7.9 and 8.9 yr.

FIG. 1. Age range distribution of fractures and cumulative number of subjects with first fracture during growth in 124 girls.

of subjects having received calcium-fortified *vs.* nonfortified foods (placebo) between mean age of 7.9 and 8.9 yr was slightly but not significantly higher in the NO-FX (56.1%) than in the FX (45.2%) group. The only significant difference between the FX and NO-FX groups was the mean age of menarche (MENA) (13.45 ± 1.11 *vs.* 12.78 ± 1.19 yr, $P = 0.003$; range 10.2–16.4 yr) (Table 1). The FX group experienced their first menstruation about 8 months later than the NO-FX group.

Fracture characteristics

Sixty-one fractures occurred in 42 of the 124 subjects. More than one fracture (two to four) was recorded in 14

girls, accounting for 34 fractures and 56% (34 of 61) of all fractures. Most fractures were localized in forearm and wrist (41%), followed by hand/fingers (13%) and arm/shoulder (7%), whereas 26% occurred at the lower limb (including, foot, ankle, tibia, and femur) and 13% at other sites. In girls having experienced more than one fracture, the upper limb was always involved. Peak fracture incidence occurred from 9–12 yr with 44.3% (27 of 61) of all fractures being recorded during this age range (Fig. 1).

Bone variables

DXA-measured aBMD

When examined at a mean age of 20.4 yr, the mean radius aBMD T-score (95% CI) of the cohort were +0.16 (−0.06 to +0.24) and +0.27 (+0.10 to +0.46) at the radial metaphysis and diaphysis, respectively (13, 36), attesting that the cohort could be considered at peak bone mass based on the reference value used in the clinical unit dedicated to the diagnosis of osteoporosis at the University Hospital of Geneva (13, 36).

At 20.4 yr of age, the mean aBMD at both the radial metaphysis and diaphysis sites were significantly lower in the FX than in the NO-FX group (Table 2). These differences remained statistically significant after adjustment for several potentially confounding variables including, age, MENA, standing height, body weight, calcium and protein intake, physical activity, and calcium or placebo randomization in an intervention trial that took place between mean age of 7.9 and 8.9 yr (Table 2). After exclusion of eight subjects with a finger or a toe fracture, mean

TABLE 2. Areal BMD, microstructure, and strength estimates of distal radius in 124 young adult women according to their fracture history

	NO-FX (n = 82)	FX (n = 42)	P^a	P^b
aBMD (mg/cm^2)				
Radial metaphysis	461 ± 52	436 ± 46	0.011	0.008
Radial diaphysis	719 ± 48	692 ± 50	0.006	0.005
vBMD (mg HA/cm^3)				
Total	337 ± 54	311 ± 58	0.015	0.032
Cortical	892 ± 45	878 ± 52	0.134	0.342
Trabecular	167 ± 35	151 ± 26	0.022	0.010
BV/TV (%)	14.0 ± 2.9	12.6 ± 2.1	0.021	0.009
Tb.N (mm^{-1})	2.00 ± 0.26	1.95 ± 0.23	0.324	0.232
Tb.Th (μm)	69.5 ± 10.0	64.5 ± 8.7	0.014	0.014
Tb.Sp (μm)	438 ± 68	454 ± 61	0.209	0.140
Tb.Sp SD (μm)	176 ± 38	187 ± 41	0.140	0.133
Ct.Th (μm)	827 ± 168	768 ± 189	0.081	0.128
CSA (mm^2)	260 ± 44	265 ± 48	0.562	0.937
Stiffness (kN/mm)	82.8 ± 15.9	75.0 ± 14.3	0.023	0.013
Estimated failure load (N)	3956 ± 735	3610 ± 651	0.028	0.013
Apparent modulus	2056 ± 400	1793 ± 486	0.006	0.046

Values are means ± SD. BV/TV, trabecular bone volume fraction; CSA, cross-sectional area; Ct.Th, cortical thickness; Tb.N, trabecular number; Tb.Sp, trabecular spacing; Tb.Th, trabecular thickness.

[a] P values between FX and NO-FX groups, without adjustment.

[b] P values between FX and NO-FX groups, after adjustment for age, MENA, height, weight, calcium and protein intakes, physical activity and calcium or placebo randomization between mean age of 7.9 and 8.9 y.
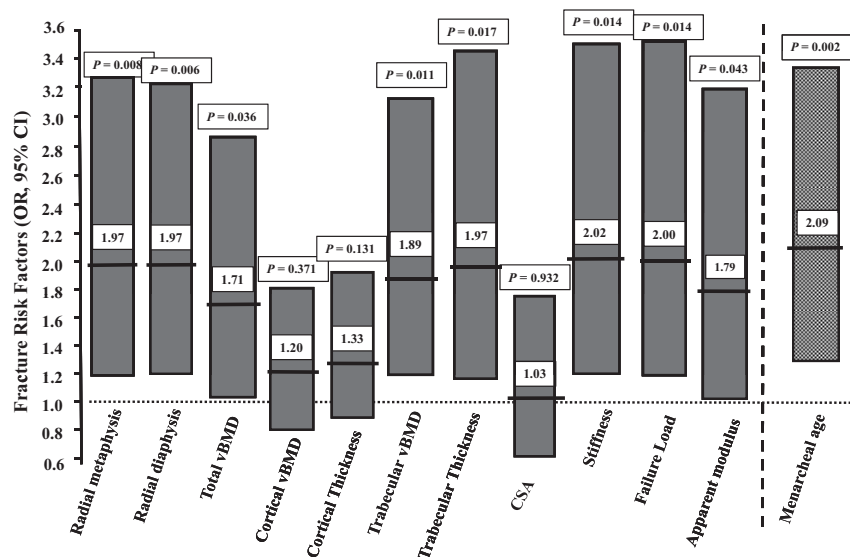
FIG. 2. Risk of fracture for 1 sd decrease in radial aBMD or in microstructure components and strength variables of the distal radius, and for 1 sd increase in MENA in 124 girls. Bone densitometric values were measured at 20.4 yr of age, once peak bone mass was attained. *Columns* are OR ± 95% CI, as evaluated by logistic regression. Statistical significance (*P*) is indicated *above each column*. CSA, Cross-sectional area.

aBMD at both the radial metaphysis and diaphysis sites remained significantly lower in the FX compared with the NO-FX group. Among the FX group, mean radial aBMD values at both radial metaphysis and diaphysis sites were very similar in women with a history of more than one fracture (two to four).

HR-pQCT-measured microstructure

The FX group, compared with the NO-FX group, displayed significantly lower total vBMD (−7.7%), trabecular bone density or trabecular bone volume fraction (−9.6 or −10.0%), and trabecular thickness (−7.2%) before and after adjustment for potential confounding factors indicated above (Table 2) as well as after exclusion of eight subjects with a finger or a toe fracture. No difference in these variables was observed in the FX group between subjects having experienced one and more than one fracture. After controlling for radial metaphysis or diaphysis aBMD, no structural parameters remained significantly different between the FX group and the NO-FX group.

μFE estimates of strength

The estimates of strength, *i.e.* stiffness (−9.2%, $P = 0.026$), failure load (−8.6%, $P = 0.028$), and apparent modulus (−11.7%, $P = 0.006$), differed between the two groups, with lower values in the FX group before and after adjustment for potential confounders (Table 2) as well as after exclusion of eight subjects with a finger or a toe fracture.

The cortical polar moment of inertia of the distal radius was lower by 3.1% ($P = 0.047$) in the FX (4045 ± 943 mm⁴) compared with the NO-FX group (4171 ± 1010 mm⁴).

aBMD, microstructure, and strength OR

As evaluated by logistic regression and expressed in terms of OR (95% CI), the risk of fracture was significantly increased for 1 sd reduction in aBMD at both the radial metaphysis and diaphysis sites (Fig. 2). The risk of fracture was also significantly higher for a decrease in the total vBMD of the distal radius (Fig. 2). Reduction in both cancellous vBMD and trabecular thickness contributed to this increased risk. The OR for radial cortical vBMD and thickness were above 1.0, but the CI overlapped unity (Fig. 2). The risk of fracture was higher with reduction in the three estimates of radial bone strength, *i.e.* stiffness, failure load, and apparent modulus (Fig. 2). At the mean age of 7.9 yr, aBMD at the radial metaphysis adjusted for age, weight, and height was predictive of fractures recorded until the mean age of 20.4 yr [OR (95% CI) = 1.58 (1.01–2.51); $P = 0.048$].

MENA and OR

In complement to the difference in MENA between the two groups presented in Table 1, the risk of fracture was significantly higher for 1 sd increase in the age at which the first menstruation was experienced (Fig. 2).

Cortical porosity

The cortical surface identifiable as pores was extremely limited, and no difference was found between the FX (0.40 ± 0.18%) and the NO-FX (0.40 ± 0.22%) group. Likewise, no significant difference was found between the two groups for the mean size of cortical pores (FX group 134 ± 11 *vs.* 134 ± 8 μm). The cortical porosity was inversely related to the cortical vBMD ($R^2 = 0.169$; $P < 0.001$) and thickness ($R^2 = 0.044$; $P = 0.050$). The slope of the regression between cortical density (x-axis, in milligrams HA per cubic centimeter) and porosity (y-axis, in percent) was not different (data not shown) between the FX group (R = −0.52; $P < 0.001$) and the NO-FX group (R = −0.40; $P < 0.001$).

Discussion

This study confirms the high prevalence of fractures during growth in healthy children and adolescents (1–5). Compared with the prevalence recorded in a male cohort living in the same community, the prevalence of girls with fractures re-

corded in this study until the age of 20.4 yr was lower (34%) than in boys (49%), despite the fact that in males the data were collected not beyond the age of 15.2 yr (6). In accordance with other reports (4, 5, 37), our study describes similar fracture rates in girls and confirms that distal forearm is the most affected skeletal site. Also consistent with several studies (1–5, 37) the highest incidence was recorded in the 9- to 12-yr range, *i.e.* in our cohort, at an age preceding by 0.5–4.5 yr the mean of MENA (13.45 yr).

An additional longitudinal recording of this healthy female cohort from 16.4 to 20.4 yr did not modify our previous results (11) documenting that the highest incidence of fracture was observed during the age range including the acceleration-deceleration in standing height gain (Fig. 1). This timing coincides with the transient delay in bone mineral accumulation when compared with the growth in standing height (2, 7, 38, 39). Sexual maturation assessment of this cohort by direct medical examination (40) indicated that the asynchrony between bone mineral mass accumulation and longitudinal growth was maximal at midpuberty (7), corresponding to the P2–P3 pubertal stage classification (41).

In our cohort, the normal range of MENA expanded from 10.2–16.4 yr, thus in conformity with other related reviews in healthy subjects (42, 43). Later pubertal maturation in girls was associated with about a 2-fold increased risk of experiencing fracture from early childhood to the onset of the third decade when peak bone mass was attained. This significant elevation in fracture risk by a factor of 2.1 was associated with reduced radial metaphysis and diaphysis aBMD.

We previously reported that, once peak bone mass was attained in this cohort, a significant inverse relationship was found between later MENA and lower radial aBMD at both diaphysis and metaphysis levels (13). The aBMD deficit was associated with reduced total and cortical vBMD of the distal radius and diminished cortical thickness without a decrease in the cross-sectional area that we interpreted as less endocortical accrual without compensatory increase in periosteal apposition (13). These structural and densitometric characteristics, which are consistent with those reported by Ackerman *et al.* (44), may explain the MENA-related risk of fractures presented in this report.

The differences in aBMD at both radial diaphysis and metaphysis levels between the FX and the NO-FX groups presented in Table 2 were close to the differences previously reported (13) between the groups experiencing later (14.0 yr) or earlier (12.1 yr) menarche. Interestingly enough, the differences of 7.7% in the total vBMD of the distal radius as assessed by HR-pQCT were identical when comparing either the later with the earlier MENA groups (13) or the FX with the NO-FX groups (Table 2). Reduction of similar magnitude was also observed in cortical

vBMD and thickness of the distal radius in relation with the presence or absence of fracture and in relation with later compared with earlier MENA as previously reported (13). However, the differences between the FX and the NO-FX groups in the cortical vBMD and thickness did not reach the level of statistical significance. Although not significant, these deficits may have contributed to the lower estimates of the strength variables in the FX group compared with the NO-FX group. The µFEA applied in the present study identified the deficits in the trabecular components of the distal radius as predominantly implicated in the risk of fracture. Calculation of OR suggested that reduction in both trabecular vBMD and thickness would be associated with a 2-fold increased risk of fracture. The magnitude of the fracture risk computed for these two trabecular variables was similar to that calculated for the corresponding differences in both radial diaphysis and metaphysis aBMD. These associations of both trabecular vBMD and strength estimates at the distal radius with an increased risk of fracture were more pronounced than those observed at the distal tibia in our cohort of healthy boys with fractures recorded until 15.2 yr of age (1–6).

From the HR-pQCT microstructure images determined at 20.4 yr of age, the µFE estimates of biomechanical properties were obtained by a compression test of the distal radius in the longitudinal direction that simulated loading due to a fall from standing height on the outstretched hand (34). This approach indicated a deficit in stiffness, corresponding to a 2-fold increase in fracture risk. Similar significant deficits and increased fracture risk were observed by modeling the failure load estimate, which was shown to be highly correlated with the stiffness of the distal radius using µFEA in the boundary conditions of loading simulation model used in this study. The apparent modulus that adjusts stiffness to the cross-sectional area variable was slightly less predictive of the fracture risk than stiffness or failure load when separately considered, but remains statistically significant.

Regarding porosity in the radial cortex, the very low cortical surface detected by the manufacture algorithm as pores was not different in the FX and NO-FX groups. This observation does not mean that during pubertal maturation, when the incidence of fracture was maximal, the degree of porosity would not have been greater in the FX than in the NO-FX groups, as suggested from a previous study on radial structure during adolescent growth (10). In this study, the percentage of porosity was as low as in the present report (about 0.4%) in healthy postpubertal subjects. However, it significantly increased during the midpuberty period (10).

Strengths and weaknesses of the study

The prospective follow-up of fracture incidence from childhood to young adult age in healthy females can be considered as a valuable aspect of our study. Likewise, this study at peak bone mass identified a deficit in distal radius variables, providing, beyond aBMD information, microstructural and biomechanical insights at the most frequently fractured skeletal site. Another contribution of this prospective study is the clear-cut identification of MENA as a risk factor for incidental fractures during skeletal development. Thus, our study corroborates the notion (11) that fractures occurring during childhood and adolescence could be markers of relatively low peak BMD associated with microarchitectural deficits that would persist during adult life and thereby increase the risk of osteoporosis.

There are limitations to this study that should be mentioned. Our study does not directly address the microstructural and mechanical resistance deficit that may be associated with the transient fragility of midpuberty when the maximal incidence of fracture is recorded. Therefore, the relation between cortical and trabecular structure and fracture incidence at the time of peak height velocity remains to be established. When microstructure and biomechanical variables are assessed, like in our current study following peak bone mass attainment, the modality of the loading test used to assess bone resistance *in vitro* by μFEA might not necessarily pertain to the most usual impact conditions resulting in forearm fractures of children and adolescents. Finally, our biomechanical analysis did not assess possible differences in the material property of the radial cortex between the FX and the NO-FX groups. This material variable, as potentially determined by adding another technical approach such as microindentation in different planes (45–47), might improve the discrimination between mechanically defective and robust bony structures in relation to the occurrence of fracture in healthy children and adolescents.

In conclusion, healthy young adult women who sustained at least one fracture during childhood and adolescence, compared with those who did not experience any fracture, had lower aBMD at the radial diaphysis and metaphysis. At the distal radius, they exhibited lower trabecular vBMD and thickness, and reduced bone strength variables, as assessed by estimating stiffness, failure load, and apparent modulus. By the end of bone development, we did not detect more extended cortical porosity in the fracture group. This study also shows that later age of menarche is associated with increased incidence of fracture during childhood and adolescence.

Acknowledgments

References

1. **Landin LA** 1983 Fracture patterns in children. Analysis of 8,682 fractures with special reference to incidence, etiology and secular changes in a Swedish urban population 1950–1979. Acta Orthop Scand Suppl 202:1–109
2. **Bailey DA, Wedge JH, McCulloch RG, Martin AD, Bernhardson SC** 1989 Epidemiology of fractures of the distal end of the radius in children as associated with growth. J Bone Joint Surg Am 71:1225–1231
3. **Jones IE, Williams SM, Dow N, Goulding A** 2002 How many children remain fracture-free during growth? a longitudinal study of children and adolescents participating in the Dunedin Multidisciplinary Health and Development Study. Osteoporos Int 13:990–995
4. **Khosla S, Melton 3rd LJ, Dekutoski MB, Achenbach SJ, Oberg AL, Riggs BL** 2003 Incidence of childhood distal forearm fractures over 30 years: a population-based study. Jama 290:1479–1485
5. **Cooper C, Dennison EM, Leufkens HG, Bishop N, van Staa TP** 2004 Epidemiology of childhood fractures in Britain: a study using the general practice research database. J Bone Miner Res 19:1976–1981
6. **Chevalley T, Bonjour JP, van Rietbergen B, Ferrari S, Rizzoli R** 2011 Fractures during childhood and adolescence in healthy boys: relation with bone mass, microstructure, and strength. J Clin Endocrinol Metab 96:3134–3142
7. **Fournier PE, Rizzoli R, Slosman DO, Theintz G, Bonjour JP** 1997 Asynchrony between the rates of standing height gain and bone mass accumulation during puberty. Osteoporos Int 7:525–532
8. **Wang Q, Alén M, Nicholson P, Lyytikäinen A, Suuriniemi M, Helkala E, Suominen H, Cheng S** 2005 Growth patterns at distal radius and tibial shaft in pubertal girls: a 2-year longitudinal study. J Bone Miner Res 20:954–961
9. **Parfitt AM** 1994 The two faces of growth: benefits and risks to bone integrity. Osteoporos Int 4:382–398
10. **Kirmani S, Christen D, van Lenthe GH, Fischer PR, Bouxsein ML, McCready LK, Melton 3rd LJ, Riggs BL, Amin S, Müller R, Khosla S** 2009 Bone structure at the distal radius during adolescent growth. J Bone Miner Res 24:1033–1042
11. **Ferrari SL, Chevalley T, Bonjour JP, Rizzoli R** 2006 Childhood fractures are associated with decreased bone mass gain during puberty: an early marker of persistent bone fragility? J Bone Miner Res 21:501–507
12. **Chevalley T, Bonjour JP, Ferrari S, Rizzoli R** 2009 The Influence of Pubertal Timing on Bone Mass Acquisition: A Predetermined Trajectory Detectable Five Years before Menarche. J Clin Endocrinol Metab 94:3424–3431

13. **Chevalley T, Bonjour JP, Ferrari S, Rizzoli R** 2008 Influence of age at menarche on forearm bone microstructure in healthy young women. J Clin Endocrinol Metab 93:2594–2601

14. **Bonjour JP, Chevalley T** 2007 Pubertal timing, peak bone mass and fragility fracture risk. IBMS BoneKEy 4:30–48

15. **Kindblom JM, Lorentzon M, Norjavaara E, Hellqvist A, Nilsson S, Mellström D, Ohlsson C** 2006 Pubertal timing predicts previous fractures and BMD in young adult men: the GOOD study. J Bone Miner Res 21:790–795

16. **Bonjour JP, Carrie AL, Ferrari S, Clavien H, Slosman D, Theintz G, Rizzoli R** 1997 Calcium-enriched foods and bone mass growth in prepubertal girls: a randomized, double-blind, placebo-controlled trial. J Clin Invest 99:1287–1294

17. **Bonjour JP, Chevalley T, Ammann P, Slosman D, Rizzoli R** 2001 Gain in bone mineral mass in prepubertal girls 3.5 years after discontinuation of calcium supplementation: a follow-up study. Lancet 358:1208–1212

18. **Chevalley T, Rizzoli R, Hans D, Ferrari S, Bonjour JP** 2005 Interaction between calcium intake and menarcheal age on bone mass gain: an eight-year follow-up study from prepuberty to postmenarche. J Clin Endocrinol Metab 90:44–51

19. **Fardellone P, Sebert JL, Bouraya M, Bonidan O, Leclercq G, Doutrellot C, Bellony R, Dubreuil A** 1991 [Evaluation of the calcium content of diet by frequential self-questionnaire]. Rev Rhum Mal Osteoartic 58:99–103 (French)

20. **Morin P, Herrmann F, Ammann P, Uebelhart B, Rizzoli R** 2005 A rapid self-administered food frequency questionnaire for the evaluation of dietary protein intake. Clin Nutr 24:768–774

21. **Boot AM, de Ridder MA, Pols HA, Krenning EP, de Muinck Keizer-Schrama SM** 1997 Bone mineral density in children and adolescents: relation to puberty, calcium intake, and physical activity. J Clin Endocrinol Metab 82:57–62

22. **Ainsworth BE, Haskell WL, Leon AS, Jacobs Jr DR, Montoye HJ, Sallis JF, Paffenbarger Jr RS** 1993 Compendium of physical activities: classification of energy costs of human physical activities. Med Sci Sports Exerc 25:71–80

23. **Boutroy S, Bouxsein ML, Munoz F, Delmas PD** 2005 In vivo assessment of trabecular bone microarchitecture by high-resolution peripheral quantitative computed tomography. J Clin Endocrinol Metab 90:6508–6515

24. **Laib A, Häuselmann HJ, Rüegsegger P** 1998 In vivo high resolution 3D-QCT of the human forearm. Technol Health Care 6:329–337

25. **Buie HR, Campbell GM, Klinck RJ, MacNeil JA, Boyd SK** 2007 Automatic segmentation of cortical and trabecular compartments based on a dual threshold technique for in vivo micro-CT bone analysis. Bone 41:505–515

26. **Burghardt AJ, Kazakia GJ, Ramachandran S, Link TM, Majumdar S** 2010 Age- and gender-related differences in the geometric properties and biomechanical significance of intracortical porosity in the distal radius and tibia. J Bone Miner Res 25:983–993

27. **Nishiyama KK, Macdonald HM, Buie HR, Hanley DA, Boyd SK** 2010 Postmenopausal women with osteopenia have higher cortical porosity and thinner cortices at the distal radius and tibia than women with normal aBMD: an in vivo HR-pQCT study. J Bone Miner Res 25:882–890

28. **MacNeil JA, Boyd SK** 2007 Accuracy of high-resolution peripheral quantitative computed tomography for measurement of bone quality. Med Eng Phys 29:1096–1105

29. **Boutroy S, Van Rietbergen B, Sornay-Rendu E, Munoz F, Bouxsein ML, Delmas PD** 2008 Finite element analysis based on in vivo HR-pQCT images of the distal radius is associated with wrist fracture in postmenopausal women. J Bone Miner Res 23:392–399

30. **Dalzell N, Kaptoge S, Morris N, Berthier A, Koller B, Braak L, van Rietbergen B, Reeve J** 2009 Bone micro-architecture and determinants of strength in the radius and tibia: age-related changes in a population-based study of normal adults measured with high-resolution pQCT. Osteoporos Int 20:1683–1694

31. **Vilayphiou N, Boutroy S, Sornay-Rendu E, Van Rietbergen B, Munoz F, Delmas PD, Chapurlat R** 2010 Finite element analysis performed on radius and tibia HR-pQCT images and fragility fractures at all sites in postmenopausal women. Bone 46:1030–1037

32. **van Rietbergen B, Weinans H, Huiskes R, Odgaard A** 1995 A new method to determine trabecular bone elastic properties and loading using micromechanical finite-element models. J Biomech 28:69–81

33. **Pistoia W, van Rietbergen B, Lochmüller EM, Lill CA, Eckstein F, Rüegsegger P** 2002 Estimation of distal radius failure load with micro-finite element analysis models based on three-dimensional peripheral quantitative computed tomography images. Bone 30:842–848

34. **Chiu J, Robinovitch SN** 1998 Prediction of upper extremity impact forces during falls on the outstretched hand. J Biomech 31:1169–1176

35. **Mueller TL, Christen D, Sandercott S, Boyd SK, van Rietbergen B, Eckstein F, Lochmüller EM, Müller R, van Lenthe GH** 2011 Computational finite element bone mechanics accurately predicts mechanical competence in the human radius of an elderly population. Bone 48:1232–1238

36. **Chevalley T, Bonjour JP, Ferrari S, Rizzoli R** 2009 Deleterious effect of late menarche on distal tibia microstructure in healthy 20-year-old and premenopausal middle-aged women. J Bone Miner Res 24:144–152

37. **Tiderius CJ, Landin L, Düppe H** 1999 Decreasing incidence of fractures in children: an epidemiological analysis of 1,673 fractures in Malmo, Sweden, 1993–1994. Acta Orthop Scand 70:622–626

38. **Faulkner RA, Davison KS, Bailey DA, Mirwald RL, Baxter-Jones AD** 2006 Size-corrected BMD decreases during peak linear growth: implications for fracture incidence during adolescence. J Bone Miner Res 21:1864–1870

39. **McKay HA, Bailey DA, Mirwald RL, Davison KS, Faulkner RA** 1998 Peak bone mineral accrual and age at menarche in adolescent girls: a 6-year longitudinal study. J Pediatr 133:682–687

40. **Theintz G, Buchs B, Rizzoli R, Slosman D, Clavien H, Sizonenko PC, Bonjour JP** 1992 Longitudinal monitoring of bone mass accumulation in healthy adolescents: evidence for a marked reduction after 16 years of age at the levels of lumbar spine and femoral neck in female subjects. J Clin Endocrinol Metab 75:1060–1065

41. **Sizonenko PC, Burr IM, Kaplan SL, Grumbach MM** 1970 Hormonal changes in puberty. II. Correlation of serum luteinizing hormone and follicle stimulating hormone with stages of puberty and bone age in normal girls. Pediatr Res 4:36–45

42. **Ducharme JR, Forest MG** 1993 Normal pubertal development. In: Betrand J, Rappaport R, Sizonenko PC, eds. Pediatric endocrinology. Physiology, pathophysiology, and clinical aspects. Baltimore: Williams, Wilkins; 372–386

43. **Parent AS, Teilmann G, Juul A, Skakkebaek NE, Toppari J, Bourguignon JP** 2003 The timing of normal puberty and the age limits of sexual precocity: variations around the world, secular trends, and changes after migration. Endocr Rev 24:668–693

44. **Ackerman KE, Nazem T, Chapko D, Russell M, Mendes N, Taylor AP, Bouxsein ML, Misra M** 2011 Bone microarchitecture is impaired in adolescent amenorrheic athletes compared with eumenorrheic athletes and nonathletic controls. J Clin Endocrinol Metab 96:3123–3133

45. **Dall'ara E, Schmidt R, Zysset P** 2012 Microindentation can discriminate between damaged and intact human bone tissue. Bone 50:925–929

46. **Reisinger AG, Pahr DH, Zysset PK** 2011 Principal stiffness orientation and degree of anisotropy of human osteons based on nanoindentation in three distinct planes. J Mech Behav Biomed Mater 4:2113–2127

47. **Zysset PK** 2009 Indentation of bone tissue: a short review. Osteoporos Int 20:1049–1055